Video Article

Harnessing the Bioorthogonal Inverse Electron Demand Diels-Alder Cycloaddition for Pretargeted PET Imaging

Thomas Reiner*[1], Jason S. Lewis[1], Brian M. Zeglis*[1]

[1]Department of Radiology, Memorial Sloan Kettering Cancer Center

*These authors contributed equally

Correspondence to: Brian M. Zeglis at zeglisb@mskcc.org

URL: http://www.jove.com/video/52335
DOI: doi:10.3791/52335

Keywords: Bioengineering, Issue 96, Positron Emission Tomography, Click Chemistry, Pretargeting, Tetrazine, *Trans*-cyclooctene, Inverse Electron Demand Diels-Alder Cycloaddition

Date Published: 2/3/2015

Citation: Reiner, T., Lewis, J.S., Zeglis, B.M. Harnessing the Bioorthogonal Inverse Electron Demand Diels-Alder Cycloaddition for Pretargeted PET Imaging. *J. Vis. Exp.* (96), e52335, doi:10.3791/52335 (2015).

Abstract

Due to their exquisite affinity and specificity, antibodies have become extremely promising vectors for the delivery of radioisotopes to cancer cells for PET imaging. However, the necessity of labeling antibodies with radionuclides with long physical half-lives often results in high background radiation dose rates to non-target tissues. In order to circumvent this issue, we have employed a pretargeted PET imaging strategy based on the inverse electron demand Diels-Alder cycloaddition reaction. The methodology decouples the antibody from the radioactivity and thus exploits the positive characteristics of antibodies, while eschewing their pharmacokinetic drawbacks. The system is composed of four steps: (1) the injection of a mAb-*trans*-cyclooctene (TCO) conjugate; (2) a localization time period during which the antibody accumulates in the tumor and clears from the blood; (3) the injection of the radiolabeled tetrazine; and (4) the *in vivo* click ligation of the components followed by the clearance of excess radioligand. In the example presented in the work at hand, a ^{64}Cu-NOTA-labeled tetrazine radioligand and a *trans*-cyclooctene-conjugated humanized antibody (huA33) were successfully used to delineate SW1222 colorectal cancer tumors with high tumor-to-background contrast. Further, the pretargeting methodology produces high quality images at only a fraction of the radiation dose to non-target tissue created by radioimmunoconjugates directly labeled with ^{64}Cu or ^{89}Zr. Ultimately, the modularity of this protocol is one of its greatest assets, as the *trans*-cyclooctene moiety can be appended to any non-internalizing antibody, and the tetrazine can be attached to a wide variety of radioisotopes.

Video Link

The video component of this article can be found at http://www.jove.com/video/52335/

Introduction

Over the last thirty years, positron emission tomography (PET) has become an indispensable clinical tool in the diagnosis and management of cancer. Antibodies have long been considered promising vectors for the delivery of positron-emitting radioisotopes to tumors due to their exquisite affinity and specificity for cancer biomarkers.[1,2] However, the relatively slow *in vivo* pharmacokinetics of antibodies mandates the use of radioisotopes with multi-day physical half-lives. This combination can yield high radiation doses to the non-target organs of patients, an important complication that is of particular clinical significance since radioimmunoconjugates are injected intravenously and therefore — unlike partial body CT scans — result in absorbed doses in every part of the body, irrespective of the interrogated tissues.

In order to bypass this issue, significant effort has been dedicated to the development of PET imaging strategies that decouple the radioisotope and the targeting moiety, thereby leveraging the advantageous properties of antibodies while simultaneously skirting their intrinsic pharmacokinetic limitations. These strategies — most often termed *pretargeting* or *multistep targeting* — typically employ four steps: (1) the administration of an antibody capable of binding both an antigen and a radioligand; (2) the accumulation of the antibody in the target tissue and its clearance from the blood; (3) the administration of a small molecule radioligand; and (4) the *in vivo* ligation of the radioligand to the antibody followed by the rapid clearance of excess radioligand.[3-8] In some cases, an additional clearing agent is injected between steps 2 and 3 in order to accelerate the excretion of any antibody that has yet to bind the tumor and remains in the blood.[5]

Broadly speaking, two types of pretargeting strategies are most prevalent in the literature. While both have proven successful in preclinical models, they also possess key limitations that have impeded their clinical applicability. The first strategy relies on the high affinity between streptavidin-conjugated antibodies and biotin-modified radiolabels; however, the immunogenicity of the streptavidin-modified antibodies has proven to be a worrisome problem with regard to translation.[5,6,9,10] The second strategy, in contrast, employs bispecific antibodies that have been genetically-engineered to bind both a cancer biomarker antigen *and* a small molecule radiolabeled hapten.[3,11-14] While this latter route is certainly creative, its broad applicability is limited by the complexity, expense, and lack of modularity of the system.

Recently, we developed and published a pretargeted PET imaging methodology based on the inverse electron demand Diels-Alder (IEDDA) cycloaddition reaction between *trans*-cyclooctene (TCO) and tetrazine (Tz; **Figure 1**).[11] While the reaction itself has been known for decades, IEDDA chemistry has experienced a renaissance in recent years as a click chemistry bioconjugation technique, as illustrated by the fascinating

Copyright © 2015 Journal of Visualized Experiments

Johns Hopkins University EX2039
GE Healthcare v. Johns Hopkins
PGR2025-00059

work of the groups of Ralph Weissleder, Joseph Fox, and Peter Conti among others.[12-15] The IEDDA cycloaddition has been applied in a wide range of settings, including fluorescence imaging with peptides, antibodies, and nanoparticles as well as nuclear imaging with both radiohalogens and radiometals.[16-26] The ligation is high yielding, clean, rapid (k_1 > 30,000 $M^{-1}sec^{-1}$), selective, and — critically — bioorthogonal.[27] And while a number of types of click chemistry — including Cu-catalyzed azide-alkyne cycloadditions, strain-promoted azide-alkyne cycloadditions, and Staudinger ligations — are bioorthogonal as well, it is the unique combination of fast reaction kinetics and bioorthogonality that makes IEDDA chemistry so well suited to pretargeting applications in whole organisms.[28,29] Along these lines, it is important to note that the recent report from our laboratories was not the first to apply IEDDA chemistry to pretargeting: the first report of pretargeted imaging with IEDDA arose from the work of Rossin, *et al.* and featured a SPECT methodology employing an ^{111}In-labeled tetrazine.[30]

As we discussed above, the pretargeting methodology has four fairly simple steps (**Figure 2**). In the protocol at hand, a pretargeted strategy for the PET imaging of colorectal cancer that employs a ^{64}Cu-NOTA-labeled tetrazine radioligand and a TCO-modified conjugate of the huA33 antibody will be described. However, ultimately the modularity of this methodology is one of its greatest assets, as the *trans*-cyclooctene moiety can be appended to any non-internalizing antibody, and the tetrazine can be attached to a wide variety of radioactive reporters.

Protocol

ETHICS STATEMENT: All of the *in vivo* animal experiments described were performed according to an approved protocol and under the ethical guidelines of the Memorial Sloan Kettering Cancer Center Institutional Animal Care and Use Committee (IACUC).

1. Synthesis of Tz-Bn-NOTA

1. In a small reaction vessel, dissolve 7 mg NH_2-Bn-NOTA (1.25×10^{-2} mmol) in 600 µl $NaHCO_3$ buffer (0.1 M, pH 8.1). Check the pH of the solution. If needed, adjust the pH of the solution to 8.1 using small aliquots of 0.1 M Na_2CO_3.
2. Add the NH_2-Bn-NOTA solution to 0.5 mg Tz-NHS (1.25×10^{-3} mmol) in a 1.7 ml microcentrifuge tube.
   NOTE: The Tz-NHS can either be weighed out dry or added from a stock solution of dry DMF or DMSO (< 50 µl).
3. Allow the resulting reaction solution to react for 30 min at RT with mild agitation.
4. After 30 min, purify the product using reversed-phase C_{18} HPLC chromatography to remove unreacted NH_2-Bn-NOTA. The NH_2-Bn-NOTA can be monitored at a wavelength of 254 nm, while the Tz-NHS and Tz-Bn-NOTA are best monitored at a wavelength of 525 nm.
   NOTE: Retention times are obviously highly dependent on the HPLC equipment setup of each laboratory (pumps, columns, tubing, *etc.*). However, to present an example, if a gradient of 0:100 MeCN/H_2O (both with 0.1% TFA) to 100:0 MeCN/H_2O over 25 min and an analytical 4.6 x 250 mm C_{18} column is used, the retention times of Tz-Bn-NOTA, Tz-NHS, and NH_2-Bn-NOTA will be around 15 min, 16.5 min, and 10 min, respectively. The product can be purified from the other reaction components in either a single run or multiple runs using a semi-preparative or preparative C_{18} HPLC column. ^{1}H-NMR, analytical HPLC, and ESI-MS are all methods that can be used to verify the purity of the completed Tz-Bn-NOTA precursor.[11]
5. Freeze the collected HPLC eluent using liquid nitrogen.
6. Wrap the frozen collection tube in opaque aluminum foil.
7. Place the frozen collection tube in a lyophilizing vessel O/N to remove the HPLC mobile phase.
8. Store the purified product (a bright pink solid) in the dark at -80 °C.
   NOTE: This is an acceptable stopping point in the procedure. The completed Tz-Bn-NOTA precursor is stable for at least 1 year under these conditions.

2. Preparation of huA33-TCO Immunoconjugate

1. In a 1.7 ml microcentrifuge tube, prepare a 1 mg/ml (2.7 mM) solution of TCO-NHS in dry DMF.
2. In a 1.7 ml microcentrifuge tube, prepare a 2 mg/ml (13.3 µM) solution of huA33 in 1 ml of phosphate buffered saline, pH 7.4 (0.01 M PO_4^{3-}, 0.154 M NaCl).
3. Using small aliquots (< 5 µl) of 0.1 M Na_2CO_3, adjust the pH of the antibody solution to 8.8-9.0. Use either pH paper or a pH meter with a microelectrode to monitor the pH, and be careful not to allow the pH to rise above pH 9.0.
4. Once the antibody solution is at the correct pH, add a volume of the TCO-NHS solution corresponding to 8 molar equivalents of the activated ester. For example, add 7.9 µl of the 1 mg/ml TCO-NHS solution (1.07×10^{-7} mol TCO-NHS) to the 1 ml of 2 mg/ml huA33 antibody solution (1.33×10^{-8} mol huA33). Do not exceed 5% DMF by volume in the solution.
5. Gently mix the solution by inverting the microcentrifuge tube several times.
6. Wrap the microcentrifuge tube in opaque aluminum foil.
7. Allow the solution to incubate for 1 hr at RT with mild agitation.
8. After 1 hr at RT, purify the resulting immunoconjugate using a pre-packed disposable size exclusion desalting column. First, rinse the size exclusion column as described by the supplier to remove any preservatives present on the column during storage. Then, add the reaction mixture to the size exclusion column, rinse the column with 1.5 ml 0.9% sterile saline, and subsequently collect the product using 2 ml of 0.9% sterile saline as the eluent.
   NOTE: This step will yield the completed huA33-TCO as a 2 ml solution.
9. Measure the concentration of the resultant huA33-TCO on a UV-Vis spectrophotometer.
10. If a higher concentration is desired, concentrate the huA33-TCO solution using a centrifugal filter unit with a 50,000 molecular weight cut-off.
    NOTE: It is important to note that while huA33 and a variety of other well-known antibodies (*e.g.,* bevacizumab, trastuzumab, cetuximab, and J591) are very tolerant of being concentrated, aggregation and precipitation can occur upon concentration in other cases. Researchers attempting this procedure with a new antibody should trust the literature or their own knowledge of the antibody in question with regard to whether or not to concentrate the antibody.
11. Store the completed huA33-TCO immunoconjugate at 4 °C in the dark.

Copyright © 2015 Journal of Visualized Experiments

NOTE: This is an acceptable stopping point in the procedure. The completed mAb-TCO conjugate should be stable for at least 3 months under these storage conditions.

3. ^{64}Cu Radiolabeling of Tz-Bn-NOTA

NOTE: This step of the protocol involves the handling and manipulation of radioactivity. Before performing these steps — or performing any other work with radioactivity — researchers should consult with their home institution's Radiation Safety Department. Take all possible steps to minimize exposure to ionizing radiation.

1. In a 1.7 ml microcentrifuge tube, prepare a 0.5 mg/ml (723 µM) solution of Tz-Bn-NOTA.
2. In a 1.7 ml microcentrifuge tube, add 10 µl of the Tz-Bn-NOTA solution (5 µg) to 400 µl of 0.2 M NH_4OAc pH 5.5 buffer.
3. In the interest of proper radiochemical note-keeping, measure and record the amount of radioactivity in the sample using a dose calibrator before and after the ensuing steps in the protocol below (3.4-3.8). This will help with the accurate determination of radiochemical yields.
4. Add 2,000 µCi (74 MBq) of ^{64}Cu to the Tz-Bn-NOTA solution.
   NOTE: Typically, [^{64}Cu]$CuCl_2$ is supplied in a small volume (< 30 µl) of 0.1 N HCl, and thus only small volumes (< 10 µl) of this stock solution are needed for the radiolabeling reaction. If larger volumes of the [^{64}Cu]$CuCl_2$ stock are needed, the radiolabeling reaction is tolerant of increasing the overall reaction volume. However, the pH of the radiolabeling reaction solution should be monitored carefully to ensure that it does not fall below pH 4.0.
5. Allow the solution to incubate for 10 min at RT with mild agitation.
6. After 10 min of incubation, purify the product using reversed-phase C_{18} HPLC chromatography. Retention times are obviously highly dependent on the HPLC equipment setup of each laboratory (pumps, columns, tubing, *etc.*). However, to present an example, if a gradient of 5:95 MeCN/H_2O (both with 0.1% TFA) to 95:5 MeCN/H_2O over 15 min is used, the retention time of ^{64}Cu-Tz-Bn-NOTA should be around 9.8 min while free, uncomplexed ^{64}Cu will elute with the solvent front at around 2-4 min.
7. Using a rotary evaporator, remove the HPLC eluent.
8. Redissolve the ^{64}Cu-Tz-Bn-NOTA product in 0.9% sterile saline.
   NOTE: Given the 12.7 hr physical half-life of ^{64}Cu, this is not an acceptable stopping point in the procedure. Perform the synthesis of ^{64}Cu-Tz-Bn-NOTA immediately prior to the injection of the radioligand, and follow Step 3.7 immediately by Step 4.5.

4. *In Vivo* Pretargeted PET Imaging

NOTE: As in Protocol Section 3, this step of the protocol involves the handling and manipulation of radioactivity. Before performing these steps researchers should consult with their home institution's Radiation Safety Department. Take all possible steps to minimize exposure to ionizing radiation.

1. In a female athymic nude mouse, subcutaneously implant 1 x 10^6 SW1222 colorectal cancer cells and allow these to grow into a 100-150 mm^3 xenograft (9-12 days after inoculation).[11]
2. Dilute an aliquot of the huA33-TCO solution from *Protocol Section 2* to a concentration of 0.5 mg/ml in 0.9% sterile saline.
3. Inject 200 µl of the huA33-TCO solution (100 µg) into the tail vein of the xenograft-bearing mouse.
4. Allow 24 hr for the accumulation of the huA33-TCO in the tumor of the mouse.
5. Dilute the ^{64}Cu-Tz-Bn-NOTA radioligand to a concentration of 1.5 mCi/ml in 0.9% sterile saline.
6. Inject 200 µl of the ^{64}Cu-Tz-Bn-NOTA radioligand solution (300 µCi; 11.1 MBq; 1.6 nmol of ^{64}Cu-Tz-Bn-NOTA, assuming a specific activity of 6.7 MBq/nmol) into the tail vein of the xenograft-bearing mice.
7. At the desired imaging time point (*e.g.,* 2, 6, 12, or 24 hr post-injection), anesthetize the mouse with a 2% isoflurane:oxygen gas mixture.
8. Place the mouse on the bed of the small animal PET scanner. Maintain anesthesia during the scan using a 1% isoflurane:oxygen gas mixture. Prior to placing the animal on the scanner bed, verify anesthesia using the toe-pinch method and apply veterinary ointment to the eyes of the mouse to prevent drying during anesthesia.
9. Acquire the PET data for the mouse via a static scan with a minimum of 20 million coincident events using an energy window of 350-700 keV and a coincidence timing window of 6 nsec. After completing the acquisition of the image, do not leave the mouse unattended and do not place it in a cage with other mice until it has regained consciousness.

Representative Results

The initial three steps of the experiment — the synthesis of Tz-Bn-NOTA, the conjugation of TCO to huA33, and the radiolabeling of the Tz-Bn-NOTA construct (**Figures 3** and **4**) — are highly reliable. In the case of the procedure above, the Tz-Bn-NOTA construct was synthesized in high yield and purity. The huA33 antibody was modified with 4.2 ± 0.6 TCO/mAb, and Tz-Bn-NOTA was radiolabeled with ^{64}Cu to yield the purified radioligand in >99% radiochemical purity, >85% decay-corrected yield, and a specific activity of ~6.7 MBq/nmol (**Figure 5**). The reactivity of the huA33-TCO conjugate and the tetrazine radioligand can be tested using radioactive instant thin layer chromatography (iTLC). This is done by mixing the radiolabeled tetrazine (100 µCi; 0.55 nmol, assuming a specific activity of 6.7 MBq/nmol) with a slight excess of huA33-TCO (50 µg; 0.66 nmol) in phosphate-buffered saline (pH 7.4) at RT for 5 min. Then, approximately 1 µCi of the solution is spotted onto a reverse-phase C_{18} TLC plate and allowed to dry. The TLC is run in 9:1 MeCN:H_2O, and the plate analyzed using a radioactive TLC plate reader. If the click reaction works as planned, the ligated ^{64}Cu-NOTA-A33 should remain at the baseline; if, on the other hand, the reaction fails, free ^{64}Cu-Tz-Bn-NOTA will appear at or near the solvent front.

Moving on to the *in vivo* imaging experiments, in the protocol described above, athymic nude mice bearing A33 antigen-expressing, SW1222 colorectal cancer xenografts were employed. Both acute biodistribution (n = 5 per time point) and PET imaging (n = 12) experiments reveal that the pretargeting strategy is capable of delineating the colorectal tumor growth with excellent image contrast and high tumor-to-background activity ratios (**Figure 6**). Uptake of the ^{64}Cu-Tz-Bn-NOTA in the tumor is apparent at early time points: 3.5% ± 0.6% ID/g and 4.1% ± 0.6 % ID/g at 1 hr and 4 hr post injection, respectively. However, at these early points, it is easily obscured by the amount of radioactivity clearing through

the intestinal tract of the mouse (11.9% ± 4.4% ID/g and 8.8% ± 3.4% ID/g in the feces at 1 hr and 4 hr p.i., respectively). Over the course of several hours, the excess radioligand clears through the feces (1.4% ± 0.5% ID/g at 24 hr p.i.), and the tumor becomes the most prominent feature in the image (4.0% ± 0.9% ID/g at 24 hr p.i.). At these later time points, the tumor is well delineated in the image, and the tumor-to-background activity ratios are quite high; for example, the strategy yields tumor:muscle ratios of 26.6 ± 6.6 at 12 hr p.i. and 27.0 ± 7.4 at 24 hr p.i. Not surprisingly, control experiments using only ^{64}Cu-Tz-Bn-NOTA, non-specific antibodies, or huA33 without conjugated TCO moieties all resulted in minimal uptake in the tumor.

As will be discussed further below, this pretargeting strategy — like all pretargeting strategies — has a number of variables that will require optimization when applied to new antibody/antigen systems. Two of the most important are the mass of mAb-TCO construct injected and the length of the interval between the injection of the mAb-TCO construct and the injection of the radioligand. If the amount of mAb-TCO conjugate is too high *or* the interval time between injections is too short, the amount of free mAb-TCO in the blood goes up and the likelihood of click reactions occurring in the blood rather than at the tumor increases. For example, in the ^{64}Cu/huA33 system discussed here, both the administration of 300 µg of huA33 (rather than 100 µg) or the use of a 12 hr interval time (rather than 24 hr) resulted in noticeable increases in the amount of radioactivity visible in the heart of the mouse (**Figure 7A** and **Figure 7B**, respectively). In both of these cases, the click reaction is still clearly occurring at the tumor, as illustrated by the amount of tumoral uptake at early time points; however, the formation of radiolabeled antibody in the blood is also apparent. While this is tempting to dismiss because the radiolabeled antibody formed in the blood will still eventually find its way to the tumor, this somewhat defeats the purpose of using a pretargeting methodology, as the radiolabeled antibody will circulate slowly before it reaches the tumor and thereby raise dose rates to non-target organs. Conversely, if too little antibody is used, the amount of uptake in the tumor will naturally suffer. Overly long interval times may also reduce levels of tumor uptake as a result of slow antibody internalization, transcyclooctene isomerization, or antibody/antigen shedding. The diagnosis of these problems is more challenging and cannot be accomplished simply through the examination of the PET data. Clearly, a delicate balance must be maintained. Therefore, it is recommended that any investigators attempting to apply this strategy to a new antibody/antigen system use large amounts of mAb-TCO construct (≥ 200 µg) and short interval times (≤ 24 hr) as starting points and optimize from there.

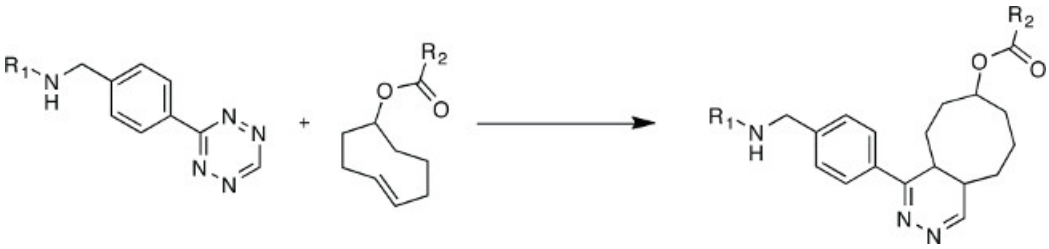

Figure 1. The inverse electron-demand Diels-Alder [4 + 2] cycloaddition click ligation between tetrazine and transcyclooctene.

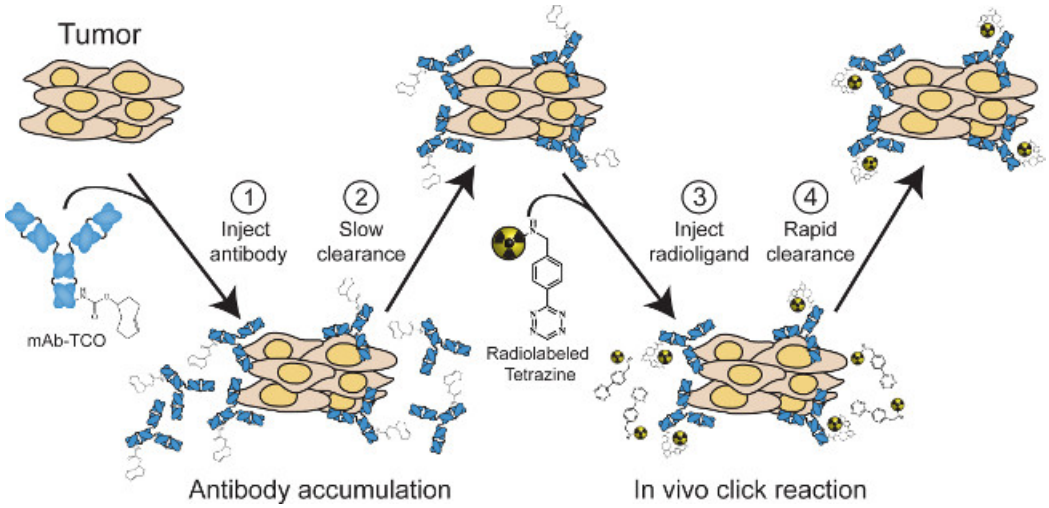

Figure 2. An illustration of the four steps of the pretargeting methodology. This figure is based on research originally published in *JNM*. Zeglis, B. M. *et al.* A pretargeted PET imaging strategy based on bioorthgonal Diels-Alder click chemistry. *Journal of Nuclear Medicine*. **54**,1389-1396 (2013). © 2013 by the Society of Nuclear Medicine and Molecular Imaging, Inc. Please click here to view a larger version of this figure.

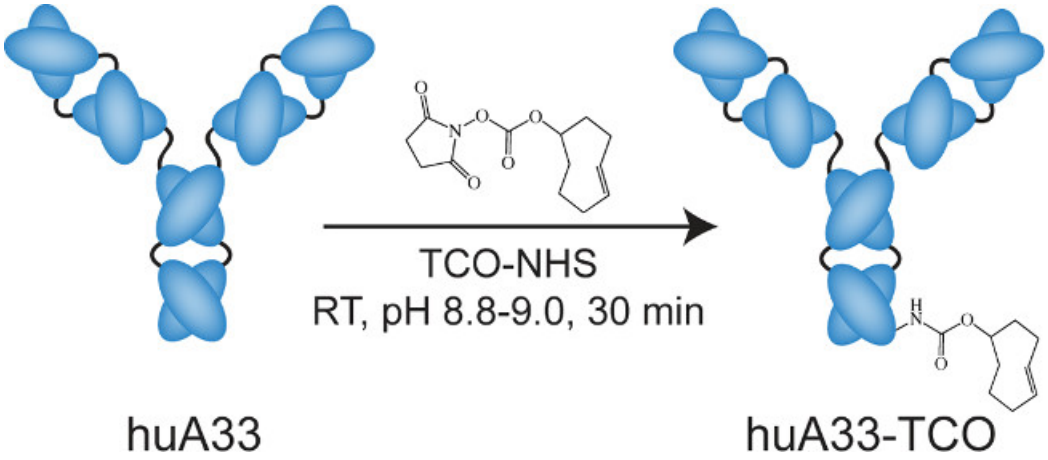

Figure 3. A scheme for the modification of huA33 with TCO-NHS.

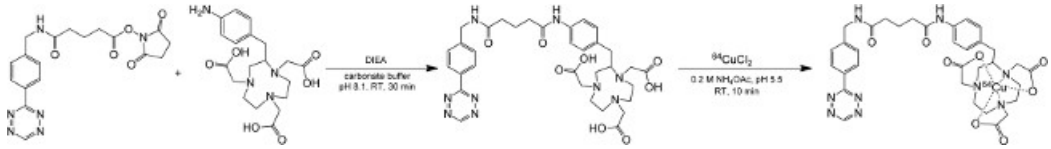

Figure 4. A scheme for the synthesis and ^{64}Cu radiolabeling of Tz-Bn-NOTA. This figure is based on research originally published in *JNM*. Zeglis, B. M. *et al.* A pretargeted PET imaging strategy based on bioorthgonal Diels-Alder click chemistry. *Journal of Nuclear Medicine*. **54**,1389-1396 (2013). © 2013 by the Society of Nuclear Medicine and Molecular Imaging, Inc. Please click here to view a larger version of this figure.

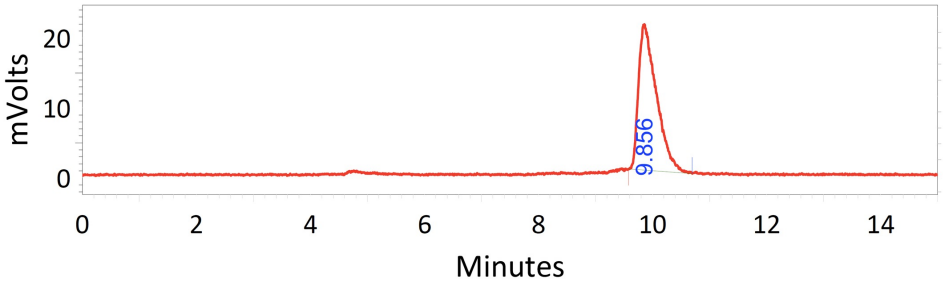

Figure 5. A radio-HPLC trace of purified ^{64}Cu-Tz-Bn-NOTA.

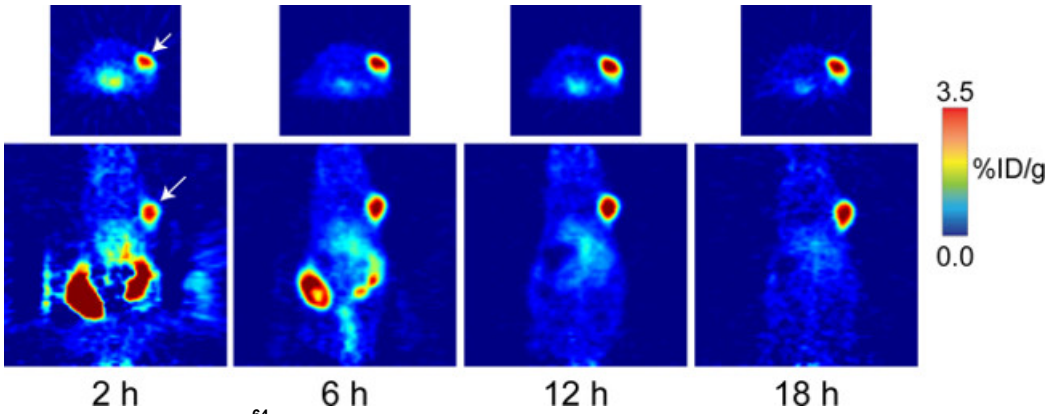

Figure 6. PET images of ^{64}Cu-Tz-Bn-NOTA/A33-TCO pretargeting strategy. Mice bearing subcutaneous SW1222 xenografts (100-150 mm^3) were administered huA33-TCO (100 µg) via tail vein injection. After 24 hr, the same mice were administered ^{64}Cu-Tz-Bn-NOTA (10.2-12.0 MBq [275-325 µCi]) via tail vein injection and subsequently imaged 2, 6, 12, and 18 hr after the administration of the radiopharmaceutical. Transverse (top) and coronal (bottom) planar images intersect the center of the tumors. High levels of uptake in the gut at early time points (*i.e.*, 2 and 6 hr) largely clear by 12 hr, leaving the tumor (white arrow) clearly delineated from all non-target tissue by 12 and 18 hr post-injection. This figure is based on research originally published in *JNM*. Zeglis, B. M. *et al.* A pretargeted PET imaging strategy based on bioorthgonal Diels-Alder click chemistry. *Journal of Nuclear Medicine*. **54**,1389-1396 (2013). © 2013 by the Society of Nuclear Medicine and Molecular Imaging, Inc. Please click here to view a larger version of this figure.

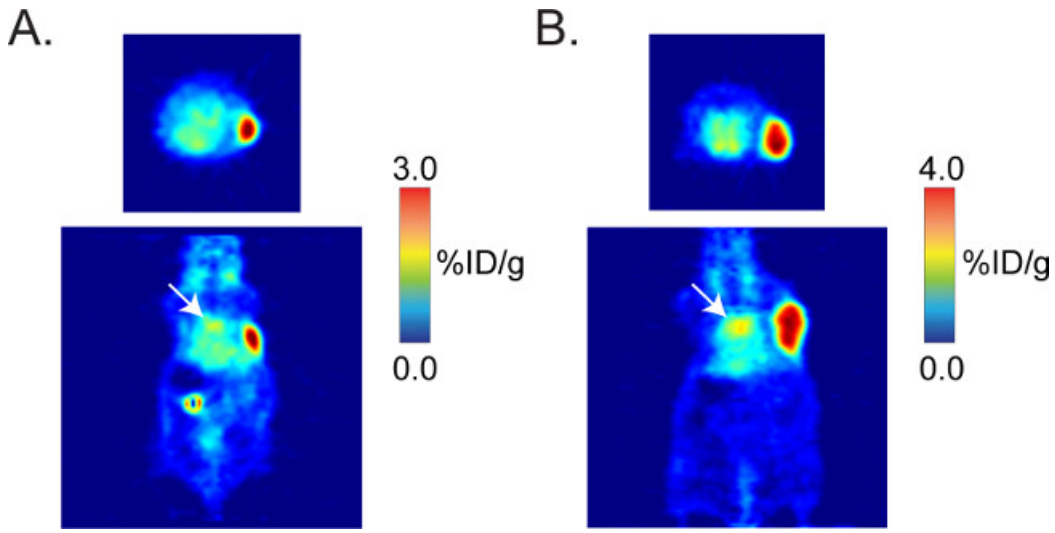

Figure 7. PET images of suboptimal pretargeting experiments. (**A**) Mice bearing subcutaneous SW1222 xenografts (100-150 mm^3, arrow) were administered huA33-TCO (100 µg) via tail vein injection. After 12 hr, the same mice were administered ^{64}Cu-Tz-Bn-NOTA (10.2-12.0 MBq [275-325 µCi]) tail vein injection. (**B**) Mice bearing subcutaneous SW1222 xenografts (100-150 mm^3, arrow) were administered A33-TCO (300 µg) via tail vein injection. After 24 hr, the same mice were administered ^{64}Cu-Tz-Bn-NOTA (10.2-12.0 MBq [275-325 µCi]) tail vein injection. In both cases, the mice were imaged 12 hr after the injection of ^{64}Cu-Tz-Bn-NOTA. In both panels, transverse (top) and coronal (bottom) planar images intersect the center of the tumors. While the pretargeting strategy clearly delineates the tumor in both cases, the results in both of these images are sub-standard compared to those displayed in **Figure 6**. In both **7A** and **7B**, there is a significant amount of background activity uptake in the heart. Under the conditions of **Figure 7A**, this is most likely the result of the huA33-TCO construct not being given enough time to localize in the tumor. Under the conditions of **Figure 7B**, this is likely a consequence of injecting too much huA33-TCO and having excess immunoconjugate still circulating in the blood even 24 hr after injection. This figure is based on research originally published in *JNM*. Zeglis, B. M. *et al.* A pretargeted PET imaging strategy based on bioorthgonal Diels-Alder click chemistry. *Journal of Nuclear Medicine*. **54**,1389-1396 (2013). 2013 by the Society of Nuclear Medicine and Molecular Imaging, Inc. Please click here to view a larger version of this figure.

Discussion

The principal advantage of this pretargeted PET imaging strategy is that it is capable of delineating tumors with target-to-background image contrast at only a fraction of the background radiation dose produced by directly labeled antibodies. For example, in the colorectal cancer imaging system described here, data from acute biodistribution experiments were employed to perform dosimetry calculations for the ^{64}Cu-based pretargeting strategy along with directly-labeled ^{64}Cu-NOTA-huA33 and ^{89}Zr-DFO-huA33. These calculations clearly illustrate the dosimetric benefits of the pretargeting system, especially when compared to the more clinically relevant ^{89}Zr-labeled antibody. The effective dose of the pretargeting strategy is 0.0124 mSv/MBq, while that of ^{89}Zr-DFO-huA33 is over 30 times higher: 0.4162 mSv/MBq. The dosimetric benefit of pretargeting is less pronounced when comparing to the ^{64}Cu-labeled antibody (0.0359 mSv/MBq), though the advantageous effect still exists.

One of the most significant strengths of this IEDDA pretargeting methodology is its modularity: the *trans*-cyclooctene can be appended to any antibody that is not internalizing, and a wide variety of cargos can be attached to the tetrazine. Indeed, our principal motivation for writing this protocol is to enable other research groups to employ this method with different antibody/antigen/radioisotope systems. Along those lines, we believe it is critical to address a number of issues that researchers should consider when adapting this methodology for other systems.

First, the selection of the antibody is tremendously important. Simply put, the antibody must be non-internalizing or internalized at a very slow rate. While the ideal kinetic parameters have yet to be determined, the antibody and the reactive *trans*-cyclooctene it carries must remain on the outside of the cell, for the internalization and sequestration of the antibody prior to the injection of the radioligand would dramatically decrease the number of *in vivo* click reactions. In the system described here, huA33 antibody targets and binds to the A33 antigen, a transmembrane glycoprotein expressed in >95% of all colorectal cancers. Importantly, it has been shown that even after binding its target, the huA33 antibody/antigen complex remains on the surface of the cell for days.[31-33] While the necessity of a non-internalizing antibody is admittedly a limitation to the strategy, a wide variety of non-internalizing antibodies are known, perhaps most notably the TAG72-targeting CC49 antibody that Rossin, *et al.* have explored in their excellent pretargeting work.[30,34,35]

Second, this pretargeting strategy — like any other — requires significant optimization. In addition to the identity of the antibody and the tetrazine radioligand, two critical variables must be considered: the amount of antibody injected and the interval time between the injections of the antibody and the radioligand. We have addressed both these variables in the *Representative Results* section above, but to reiterate briefly, if either too much antibody or too short an interval time is employed, significant amounts of mAb-TCO conjugate will remain in the blood at the time of the injection of the radioligand. This, in turn, will result in the *in vivo* click ligation occurring in the blood rather than at the tumor, forming circulating, radiolabeled antibody that will only slowly accumulate in the tumor over time. Conversely, if either too little antibody or too long an interval time is employed, the final amount of radioactivity in the tumor will be suboptimal. In our opinion, performing rigorous imaging, or preferably, acute biodistribution experiments with the directly labeled antibody itself prior to any pretargeting experiments is the most reliable way to learn about the amount of antibody needed and the ideal interval time after the initial injection of antibody construct. For different injected masses of radiolabeled mAb, these experiments will provide concrete data on both the clearance of the radioimmunoconjugate from the blood and its accumulation in the tumor, allowing for the selection of the most promising conditions for the pretargeting experiments.

Copyright © 2015 Journal of Visualized Experiments

Finally, the pharmacokinetics of the tetrazine-based radioligand must be considered when choosing a suitable radioisotope. In the system described here, the radiolabeled Tz-Bn-NOTA moiety is excreted from the body via the gut with a biological half-life of approximately 3-4 hr, making ^{64}Cu the positron-emitting radioisotope with the most complementary physical half-life. Unfortunately, the biological half-life of the tetrazine moiety is too long for it to be compatible with the more rapidly decaying radiometal ^{68}Ga ($t_{1/2}$ = 68 min). In this case, any radioactivity in the tumor would decay through several half-lives before the excess radioligand finished clearing from the body. As a result, images would have to be acquired at early time points, when tumor-to-background activity ratios remain low.[36] Ideally, future generations of tetrazine radioligands would be engineered — perhaps via PEGylation, glycation, or other means — to excrete from the body more quickly. This would allow for radiolabeling with more rapidly decaying radioisotopes such as ^{68}Ga and ^{18}F, which would in turn further enhance the dosimetric benefits of the pretargeted imaging strategy. Ultimately, as researchers adapt this technology for use with other radioisotopes for imaging (*e.g.,* ^{124}I, ^{111}In, ^{18}F, ^{89}Zr, ^{68}Ga, *etc.*) or therapy (*e.g.,* ^{89}Y, ^{177}Lu, ^{225}Ac, ^{125}I, *etc.*), new tetrazine-based ligands will need to be developed to incorporate different chelators or radiolabeling prosthetic groups. The thorough investigation of the pharmacokinetics of these novel constructs will be essential to ensuring advantageous matches between the clearance properties of the ligands and the physical half-life of the radionuclides.

In the end, we very much hope that other investigators see the promise of this pretargeting technology and employ it with new antibody/antigen systems. While the preceding paragraphs illustrate that this adaptation process may not always be simple, it is our belief that this methodology could have a significant impact on nuclear imaging, targeted radionuclide therapy, and beyond.

Disclosures

The authors have nothing to disclose.

Acknowledgements

The authors thank Prof. Ralph Weissleder, Dr. Pat Zanzonico, and Dr. NagaVaraKishore Pillarsetty for helpful conversations and the NIH for funding (BMZ: 1K99CA178205-01A1)

References

1. Wu, A. M. Antibodies and antimatter: The resurgence of immuno-PET. *Journal of Nuclear Medicine.* **50**, 2-5, doi:10.2967/jnumed.108.056887 (2009).
2. Zeglis, B. M., & Lewis, J. S. A practical guide to the construction of radiometallated bioconjugates for positron emission tomography. *Dalton Transactions.* **40**, 6168-6195, doi:10.1039/c0dt01595d (2011).
3. Hollander, N. Bispecific antibodies for cancer therapy. *Immunotherapy.* **1**, 211-222, doi:10.2217/1750743X.1.2.211 (2009).
4. Liu, G. *et al.* Tumor pretargeting in mice using 99mTc-labeled morpholino, a DNA analog. *Journal of Nuclear Medicine.* **43**, 384-391 (2002).
5. Boerman, O. C., van Schaijk, F. G., Oyen, W. J. G., & Corstens, F. H. M. Pretargeted radioimmunotherapy of cancer: Progress step by step. *Journal of Nuclear Medicine.* **44**, 400-411 (2003).
6. Goldenberg, D. M., Sharkey, R. M., Paganelli, G., Barbet, J., & Chatal, J. F. Antibody pretargeting advances cancer radioimmunodetection and radioimmunotherapy. *Journal of Clinical Oncology.* **24**, 823-834, doi:10.1200/JCO.2005.03.8471 (2006).
7. Sharkey, R. M., Chang, C. H., Rossi, E. A., McBride, W. J., & Goldenberg, D. M. Pretargeting: taking an alternate route for localizing radionuclides. *Tumor Biology.* **33**, 591-600, doi:10.1007/s13277-012-0367-6 (2012).
8. Sharkey, R. M. *et al.* Improving the delivery of radionuclides for imaging and therapy of cancer using pretargeting methods. *Clinical Cancer Research.* **11**, 7109-7121, doi:10.1158/1078-0432.CCR-1004-0009 (2005).
9. Schultz, J. *et al.* A tetravalent single-chain antibody-streptavidin fusion protein for pretargeted lymphoma therapy. *Cancer Research.* **60**, 6663-6669 (2000).
10. Lewis, M. R. *et al. In vivo* evaluation of pretargeted 64Cu for tumor imaging and therapy. *Journal of Nuclear Medicine.* **44**, 1284-1292 (2003).
11. Zeglis, B. M. *et al.* A pretargeted PET imaging strategy based on bioorthgonal Diels-Alder click chemistry. *Journal of Nuclear Medicine.* **54**, 1389-1396, doi:10.2967/jnumed.112.115840 (2013).
12. Blackman, M. L., Royzen, M., & Fox, J. M. Tetrazine ligation: fast bioconjugation based on inverse electron demand Diels-Alder reactivity. *Journal of the American Chemical Society.* **130**, 13518-13519, doi:10.1021/ja8053805 (2008).
13. Devaraj, N. K., Upadhyay, R., Hatin, J. B., Hilderbrand, S. A., & Weissleder, R. Fast and sensitive pretargeted labeling of cancer cells through a tetrazine/trans-cyclooctene cycloaddition. *Angewandte Chemie-International Edition.* **48**, 7013-7016, doi:10.1002/anie.200903233 (2009).
14. Devaraj, N. K., & Weissleder, R. Biomedical applications of tetrazine cycloadditions. *Accounts of Chemical Research.* **44**, 816-827, doi:10.1021/ar200037t (2011).
15. Devaraj, N. K., Weissleder, R., & Hilderbrand, S. A. Tetrazine-based cycloadditions: application to pretargeted live cell imaging. *Bioconjugate Chemistry.* **19**, 2297-2299, doi:10.1021/bc8004446 (2008).
16. Keliher, E. J., Reiner, T., Turetsky, A., Hilderbrand, S., & Weinberg, R. A. High-yielding, two-step 18F labeling strategy for 18F-PARP1 inhibitors. *ChemMedChem.* **6**, 424-427, doi:10.1002/cmdc.201000426 (2011).
17. Reiner, T., Earley, S., Turetsky, A., & Weissleder, R. Bioorthogonal small-molecule ligands for PARP1 imaging in living cells. *ChemBioChem.* **11**, 2375-2377, doi:10.1002/cbic.201000477 (2010).
18. Reiner, T., Keliher, E. J., Earley, S., Marinelli, B., & Weissleder, R. Synthesis and *in vivo* imaging of a 18F-labeled PARP1 inhibitor using a chemically orthogonal scavenger-assisted high-performance method. *Angewandte Chemie International Edition.* **50**, 1922-1925, doi:10.1002/anie.201006579 (2011).
19. Taylor, M. T., Blackman, M., Dmitrenko, O., & Fox, J. M. Design and synthesis of highly reactive dienophiles for the tetrazine-trans-cyclooctene ligation. *Journal of the American Chemical Society.* **133**, 9646-9649, doi:10.1021/ja201844c (2011).
20. Selvaraj, R. *et al.* Tetrazine-trans-cyclooctene ligation for the rapid construction of integrin alpha(v)beta(3) targeted PET tracer based on a cyclic RGD peptide. *Bioorganic and Medicinal Chemistry Letters.* **21**, 5011-5014, doi:10.1016/j.bmcl.2011.04.116 (2011).

Copyright © 2015 Journal of Visualized Experiments

21. Liu, S. *et al.* Efficient 18F labeling of cysteine-containing peptides and proteins using tetrazine-trans-cyclooctene ligation. *Molecular Imaging.* **12**, 121-128 (2013).
22. Han, H. S. *et al.* Development of a bioorthogonal and highly efficient conjugation method for quantum dots using tetrazine-norbornene cycloaddition. *Journal of the American Chemical Society.* **132**, 7838-7839, doi:10.1021/ja101677r (2010).
23. Zeglis, B. M. *et al.* Modular strategy for the construction of radiometalated antibodies for positron emission tomography based on inverse electron demand Diels-Alder click chemistry. *Bioconjugate Chemistry.* **22**, 2048-2059, doi:10.1021/bc200288d (2011).
24. Zeng, D., Zeglis, B. M., Lewis, J. S., & Anderson, C. J. The growing impact of bioorthogonal click chemistry on the development of radiopharmaceuticals. *Journal of Nuclear Medicine.* **54**, 829-832, doi:10.2967/jnumed.112.115550 (2013).
25. Reiner, T., & Zeglis, B. M. The inverse electron demand Diels-Alder reaction in radiochemistry. *Journal of Labeled Compounds and Radiopharmaceuticals.* **57**, 285-290, doi:10.1002/jlcr.3149 (2014).
26. Li, Z. *et al.* Tetrazine-trans-cyclooctene ligation for the rapid construction of 18-F labeled probes. *Chemical Communications.* **46**, 8043-8045, doi:10.1039/c0cc03078c (2010).
27. Karver, M. R., Weissleder, R., & Hilderbrand, S. A. Synthesis and evaluation of a series of 1,2,4,5-tetrazines for bioorthogonal conjugation. *Bioconjugate Chemistry.* **22**, 2263-2270, doi:10.1021/bc200295y (2011).
28. Sletten, E. M., & Bertozzi, C. R. Bioorthogonal chemistry: fishing for selectivity in a sea of functionality. *Angewandte Chemie International Edition.* **48**, 6973-6998, doi:10.1002/anie.200900942 (2009).
29. Bosch, S. M. *et al.* Evaluation of strained alkynes for Cu-free click reaction in live mice. *Nuclear Medicine and Biology.* **40**, 415-423, doi:10.1016/j.nucmedbio.2012.12.006 (2013).
30. Rossin, R. *et al. In vivo* chemisry for pretargeted tumor imaging in live mice. *Angewandte Chemie International Edition.* **49**, 3375-3378, doi:10.1002/anie.200906294 (2010).
31. Ackerman, M. E. *et al.* A33 antigen displays persistent surface expression. *Cancer Immunology and Immunotherapy.* **57**, 1017-1027, doi:10.1007/s00262-007-0433-x (2008).
32. Carrasquillo, J. A. *et al.* 124I-huA33 antibody PET of colorectal cancer. *Journal of Nuclear Medicine.* **52**, 1173-1180, doi:10.2967/jnumed.110.086165 (2011).
33. Sakamoto, J. *et al.* A phase I radioimmunolocalization trial of humanized monoclonal antibody huA33 in patients with gastric carcinoma. *Cancer Science.* **97**, 1248-1254, doi:10.1111/j.1349-7006.2006.00324.x (2006).
34. Rossin, R., Lappchen, R., van den Bosch, S. M., LaForest, R., & Robillard, M. S. Diels-Alder reaction for tumor pretargeting: *In vivo* chemistry can boost tumor radiation dose compared with directly labeled antibody. *Journal of Nuclear Medicine.* **54**, 1989-1995, doi:10.2967/jnumed.113.123745 (2013).
35. Rossin, R. *et al.* Highly reactive trans-cyclooctene tags with improved stability for Diels-Alder chemistry in living systems. *Bioconjugate Chemistry.* **34**, 1210-1217, doi:10.1021/bc400153y (2014).
36. Emmetiere, F. *et al.* 18F-labeled-bioorthogonal liposomes for *in vivo* targeting. *Bioconjugate Chemistry.* **24**, 1784-1789, doi:10.1021/bc400322h (2013).

Copyright © 2015 Journal of Visualized Experiments